International Journal of Aviation Science and Engineering
e-ISSN: 2715-6958 p-ISSN: 2721-5342
AVIA

Original Article

Analysis of Low-Noise Amplifier Design for 1 GHz IoT Water Monitoring System

Fadil Hamdani*[1], Misfa Susanto[1] and Heriansyah[2, 3]

[1] Department of Electrical Engineering, Faculty of Engineering, Universitas Lampung. Jl. Prof. Dr. Sumantri Brojonegoro No. 1, Bandar Lampung, Indonesia
[2] Department of Electrical Engineering, Faculty of Industrial Technology, Institut Teknologi Sumatera. Jl. Terusan Ryacudu, Kab. Lampung Selatan 35365, Indonesia
[3] Department of Computer Science, Johannes Kepler University, Linz, Austria

* Correspondence: fadil.hamdani@eng.unila.ac.id

Received: 15 August 2024; Accepted: 7 October 2024; Published: 10 December 2024

The Internet has dramatically accelerated the development of machine-to-machine communication technologies, enabling the remote monitoring and control of water treatment processes. A key example of this is the Internet of Things (IoT)-based Water Quality Management (WQM) systems, which utilize wireless sensors to monitor environmental parameters in real-time. These sensors are connected to a central gateway that aggregates and transmits data, facilitating timely interventions when water quality deviates from standards. The use of wireless communication minimizes installation challenges and environmental disruption. However, signal attenuation, particularly in Ultra High Frequency (UHF) bands over water, presents a challenge due to factors like temperature variations, antenna height, and surface roughness. UHF signals, while favorable for IoT applications due to their high data throughput and low power consumption, face propagation limitations over water surfaces. Despite these challenges, UHF's ability to penetrate structures and support large networks makes it a viable choice for IoT in aquatic environments. This paper explores the design of low-noise amplifiers (LNAs) to mitigate signal attenuation in IoT systems for WQM, with a focus on enhancing signal integrity while maintaining low power consumption. By optimizing LNAs, the study aims to address the unique communication challenges posed by water environments, ensuring the reliable and efficient operation of WQM systems.

Keywords: Internet of Things; Water Quality Monitoring; Ultra High Frequency; Signal attenuation; Low Noise Amplifier.

1. Introduction

The Internet has significantly propelled the advancement of applications that are intrinsically dependent on its foundational infrastructure, as illustrated by machine-to-machine communication technologies that facilitate the effective remote oversight and regulation of water treatment processes. This specific framework exemplifies a noteworthy case of the practical application of Internet of Things (IoT) technology within the expansive realm of Water Quality Management (WQM) systems, demonstrating how sophisticated connectivity can augment environmental monitoring [1]. The architecture of this system generally entails the installation of numerous sensors that are wirelessly interconnected to a central gateway, which is tasked with aggregating data from these sensors and subsequently transmitting this information to users via established internet connections [2][3]. However, it is imperative to acknowledge that within the domain of wireless communication, the transmitted signals experience considerable path attenuation as they traverse the diverse channels of wireless transmission, which may adversely affect the fidelity of the data being transmitted [4] .

The propagation of Ultra High Frequency (UHF) signals over water surfaces presents unique challenges and opportunities due to the distinct environmental and physical characteristics of aquatic environments. Ultra High Frequency signals range from 300 MHz to 3 GHz and are widely used for television broadcasting, mobile phones, GPS, and wireless communication technologies. This frequency band is advantageous for high data rates and reduced interference; however, its propagation over water is impacted by several factors, such as temperature variations, antenna height, and surface roughness [5]. Due to the relatively short wavelength of UHF signals, they tend to follow a line-of-sight path, which limits their effective range over flat water surfaces, especially in comparison to lower frequency bands [6]. The curvature of the Earth can cause the signal to drop off at the radio horizon, typically 30–50 kilometers away, depending on antenna height. However, over water, reflections and ducting phenomena caused by temperature and humidity layers can extend the signal range beyond the visual horizon. This makes UHF propagation over water both unpredictable and occasionally more far-reaching under the right atmospheric conditions. [7]

The UHF band is increasingly being adopted for Internet of Things (IoT) applications due to its favorable characteristics for short-to-medium range communications, reliability, and ability to support high data throughput [8] [9] [10]. The transition from terrestrial to marine environments induces distinct effects on signal propagation, varying by frequency and antenna elevation [11][12]. Elevated frequencies, combined with increased antenna heights, may alleviate certain propagation obstacles encountered over aquatic surfaces. The irregularity of the oceanic surface can induce scattering of sub-GHz signals, thereby influencing both path loss and the power delay profile [13][14].

To effectively alleviate the issue of signal attenuation that may occur during transmission, the received signals are subjected to a process of amplification through the utilization of low noise amplifiers, commonly referred to as LNAs, which are specifically designed to not only enhance the overall strength of the signal but also to simultaneously minimize the potential introduction of any unwanted extraneous additive noise that could interfere with the clarity and integrity of the transmitted information [15]. In this research, we conduct a thorough investigation of the design principles governing LNAs intended for operation in the receiver side of IoT systems, developed explicitly for Water Quality Monitoring (WQM) applications. This application is characterized not only by the system's operating frequency but also by stringent low-power consumption constraints

2. Literature Review

In aquatic environments, monitoring water quality using IoT-based systems requires careful consideration of the communication technologies and bandwidth involved. The minimum bandwidth required for IoT-based wireless water quality monitoring systems depends on various factors, including the types of sensors used, data transmission technologies, and the system architecture. These systems are typically designed to monitor parameters such as pH, turbidity, temperature, and conductivity. The choice of communication technology is critical in determining the system's bandwidth requirements.

The low energy usage and long-range functionality of LoRa (Long Range) technology make it highly suitable for transmitting real-time data across large areas, such as reservoirs, without the need for high bandwidth. LoRa operates in unlicensed frequency bands, typically around 868 MHz in Europe and 915 MHz in the US, but globally it functions near 1 GHz. However, the efficiency of long-range communication, such as LoRa, is influenced by various propagation factors, including terrain and obstacles. This is where models like the two-ray model come into play.

The two-ray model extends the basic Free Space Path Loss (FSPL) model by considering not only the direct line-of-sight (LOS) path but also a reflected path from the ground, which depends on the heights of the transmitting and receiving antennas. The model accounts for the ground reflection coefficient (R), and the full two-ray model is described by Equation 1.

$$P_r = P_t\left(\frac{\lambda}{4\pi}\right)^2 \left|\frac{\sqrt{G_r G_t}}{B} + R\,\frac{\sqrt{G_t G_r}\,e^{-j\left(\frac{2\pi(A-B)}{\lambda}\right)}}{A}\right|^2 \tag{1}$$

where, h_t denotes the height of the transmitting antenna (in meters), h_r is the height of the receiving antenna (in meters), and R represents the ground reflection coefficient. The parameters A and B are defined as $A = \sqrt{d^2 + (h_t + h_r)^2}$ and $B = \sqrt{d^2 + (h_t - h_r)^2}$, respectively. A value of $R = -1$ indicates a perfectly reflecting ground, whereas $R = 0$ corresponds to a non-reflecting ground surface (zero ground reflection)

Considering the propagation environment depicted in Figure 1, with sensors located at various points on the water surface, we focus on a monitoring scheme where the traffic flows in the uplink direction.

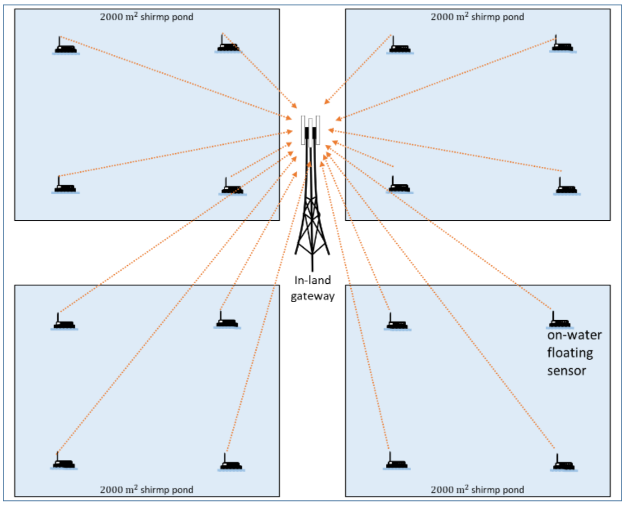

Figure 1. Environment setup for over-water wireless transmission

Using Equation 1, we can predict the received signal power. The sensor antenna height is assumed to be 10 cm, while the gateway antenna height is 4 m. The sensor transmits at a minimum power of 1 mW (0 dBm), with a 1 dB transmitter antenna gain and a 2 dB receiver antenna gain. The resulting received signal power is shown in Figure 2, where for an operating frequency of 1 GHz, the received signal is approximately -77.31 dBm.

Understanding the propagation characteristics of sub-GHz signals over long distances, particularly through models such as the two-ray model, has provided a foundation for optimizing receiver performance. A critical component in the receiver chain is the LNA, which amplifies weak long-range signals while introducing minimal additional noise. Positioned at the receiver front end, the LNA is vital for preserving signal integrity, ensuring that even distance-attenuated and reflection-degraded signals remain strong and clear for further processing. Key design considerations for LNAs include Noise Figure (NF), Gain, S-parameters (S11, S21, S12, S22), and stability, all of which significantly influence overall system performance. The Input Reflection Coefficient (S11) indicates the percentage of the input signal that is reflected due to impedance mismatches at the input interface. Minimizing S11 is key to ensuring optimal power transfer into the LNA, while the Gain (S21) reflects the amplifier’s ability to boost the signal.

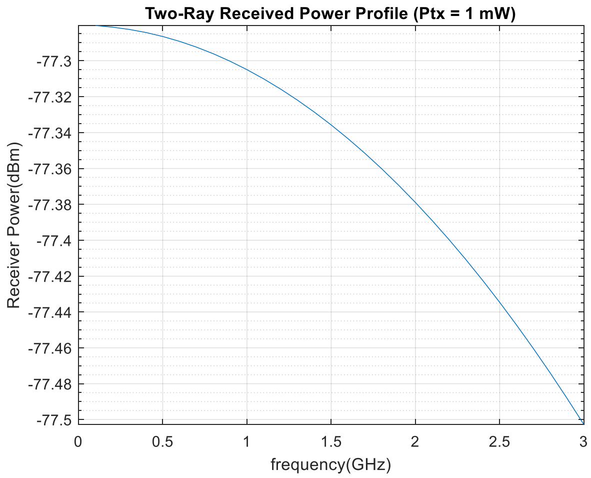

Figure 2. Received Power profile of the Two-ray model

A reduced S11 value, typically expressed in logarithmic units known as decibels (dB), signifies improved input matching, which is crucial for maximizing the transfer of signal power to the amplifier. Analogous to S11, the Output Reflection Coefficient (S22) pertains to the output port and quantifies the degree of reflection occurring from the load for the output signal.

Attaining low S22 values is crucial for reducing signal loss and enhancing overall system efficacy, particularly in high-frequency domains where even minute reflections may precipitate considerable deterioration in signal integrity. Beyond S11 and S22, the Transmission Coefficient or Forward Gain (S21) is instrumental in defining the performance metrics of the amplifier, as it measures the proportion of power transmitted from the input to the output. S21 characterizes the intrinsic amplification of the LNA and represents one of the most pivotal parameters. An elevated S21 value guarantees enhanced signal amplification, which is vital for the processing of weak signals in IoT applications such as Water Quality Monitoring. The Reverse Isolation parameter (S12) quantifies the extent of signal leakage from the output back to the input. Effective isolation, characterized by a low S12 value, is paramount in ensuring that the LNA does not compromise the overall system performance by inducing feedback or oscillatory behavior [16] [17]. The Noise Figure (NF) represents a crucial metric that indicates the deterioration of the signal-to-noise ratio as it propagates through the amplifier, thereby affecting the overall sensitivity and effectiveness in low-power applications. The Noise Figure serves as a fundamental criterion in low-noise amplifiers that evaluates the diminution of the signal-to-noise ratio (SNR) as a signal advances through the amplifier. [18] [19]

3. Methodology

To achieve optimal performance in the receiver chain, particularly for weak signals, the design of the low-noise amplifier is critical. The LNA must not only amplify the incoming signal but also maintain a low noise figure to ensure minimal signal degradation. The design methodology of the LNA involves several key steps, each aimed at ensuring that the amplifier meets the stringent performance requirements necessary for reliable operation. The design process begins with DC analysis, where the biasing conditions of the transistor are determined. Proper biasing ensure that the transistor operates in its optimal region, providing sufficient gain without introducing excessive noise or instability. This step is followed by the bias circuit design for maintaining the desired operating point under varying conditions such as temperature and supply voltage fluctuations.

The next step is to perform a stability analysis, as ensuring stability is paramount. Unstable amplifiers can lead to oscillations, especially at high frequencies. Techniques such as the use of feedback or loading networks are employed to maintain stability across the desired frequency range. After stability is confirmed, the next step involves optimizing the matching network design. Impedance matching is essential to maximize power transfer and minimize signal reflection, as indicated by the S-parameters, particularly the input reflection coefficient (S11). Both the input and output matching networks are designed to achieve low reflection and high gain across the operating frequency band. The performance optimization stage fine-tunes the LNA design to balance key parameters such as noise figure, gain, bandwidth, and linearity. The amplifier design parameters are provided in Table 2.

Table 2. Amplifier Specifications

No	Parameters	Values
1	Target operating Frequency	1 GHz
2	Target Gain	> 12 dB
3	Return Loss	< – 15 dB
4	Target DC Power consumption	< 50 mW
5	Transistor frequency range	0.5 – 6 GHz
6	Transistor Type	Low-Noise GaAs FET
7	Transistor Ambient Temperature	25°C

The ambient temperature (TA) of 25°C refers to the temperature of the surrounding environment where the transistor is operating, which is the standard reference temperature (room temperature) used for specifying electrical characteristics of semiconductors, including transistors. The behavior of the transistor may change when the ambient temperature is higher or lower than this reference.

The DC analysis of the transistor, as shown in Figure 3, highlights key elements in the LNA design. At the center is the "LNA" block, representing the amplifier being tested. The input port, labeled RFin, is where the RF signal enters, while RFout is the output port from which the amplified signal is delivered. The source, V_1Tone (SRC2), provides a sinusoidal RF input signal at a frequency of 1 GHz with an amplitude of 1 mV in polar form, which is the operating frequency for this LNA. V_DC (SRC1) represents the DC bias for the amplifier, set at 10V to power the circuit. A 50-ohm load resistor is placed at the output to simulate typical load impedance in RF systems.

The simulation setup includes Harmonic Balance (HB1), a method used in RF design to analyze the steady-state behavior of nonlinear circuits, including the LNA, by solving in the frequency domain. The primary operating frequency is set at 1 GHz, and the simulator considers up to the 4^{th} harmonic to account for nonlinear effects.

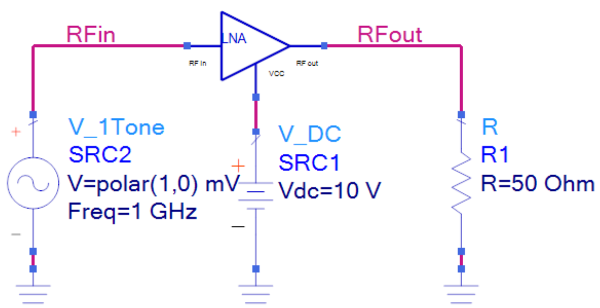

Figure 3. DC analysis of the transistor

In the context of the transistor's DC analysis, the V polar(1,0) mV refers to the input RF signal fed into the LNA. This signal is defined in polar coordinates, where 1 mV represents the amplitude and 0 represents the phase angle in degrees. The frequency of this signal is 1 GHz, which corresponds to the operating frequency of the LNA. This RF signal is a weak input, such as from a wireless sensor node, that the LNA is designed to amplify. The Vdc 10V is the DC bias voltage applied to the transistor in the LNA circuit. This bias voltage provides the necessary operating conditions for the transistor, ensuring that it operates in the correct region. The DC bias ensures that the transistor remains in its active region, enabling it to amplify the small RF signal. Without proper biasing, the transistor could either be in cutoff, where no amplification occurs, or in saturation, where the transistor is fully on, which also prevents proper amplification.

4. Discussion

The layout of the Low Noise Amplifier developed in this study is illustrated in Figure 4. The amplifier section includes several elements, with multiple stages of amplification represented by components microstrip line (MLIN) microstrip T-junction (MTee). These components indicate that the circuit operates within the RF (radio frequency) or microwave range. Active components, such as the AT41411, represent the transistor which is utilized to amplify the incoming signal. The matching network is represented by the MLIN and MTee sections, functioning as an impedance matching network to ensure proper signal transfer between stages. Capacitors and inductors are positioned along the transmission paths, serving as matching elements at high frequencies.

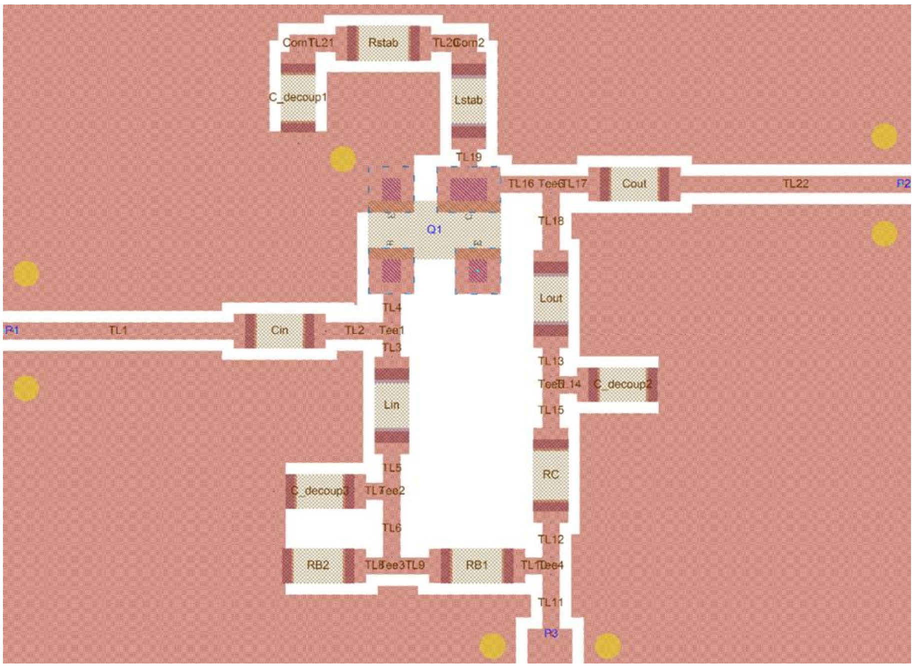

Figure 4. LNA Layout

The biasing network is illustrated with resistors and capacitors located near the transistor, along with DC blocks or bias tees that indicate the presence of a biasing network to establish the correct operating point of the transistor. The DC Block capacitor, marked with components C, is used to prevent DC from affecting the RF signal path. The input and output ports are designed for signal transmission or reception, configured with 50-ohm impedance at each port, which is standard in RF circuits. The grounding arrangement and via pads indicate the presence of ground connections to maintain stability and isolation for the RF circuit.

The layout comprises several key areas. The component area includes labels such as "Rstab" and "C_decoup1," which denote regions housing essential components. These labels correspond to resistors (Rstab), capacitors (C_decoup) utilized for stabilization and decoupling within the LNA design. The amplification paths, indicated by various "TL" labels (for instance, TL16, TL19, etc.), represent transmission lines vital for signal routing and impedance matching. The "Q1" label at the center likely identifies the primary transistor or active device within the LNA, serving as the core amplification element.

Input and output components are denoted by Cin and Cout, referring to input and output capacitors, respectively. These components are crucial for blocking DC while allowing RF signals to pass through. Areas marked "L," representing inductors, such as "Lout," indicate positions for inductors used in impedance matching or as part of tank circuits. The biasing network, characterized by resistors and capacitors around the edges, such as "Rstab" and "C_decoup1," is integral to the biasing and stabilization of the amplifier. Resistors provide the correct operating bias for the transistor, while capacitors filter out noise or undesirable frequencies.

Components "Rstab" are used to ensure stability across the entire frequency range of operation, while transmission lines (TL) and inductors offer precise matching for the common 50-ohm impedance environment found in RF systems. The two yellow circles represent connection points that ensure the circuit is properly grounded, preventing unwanted noise or instability in the LNA design. The gain and performance of the amplifier across frequencies up to 4 GHz are characterized in Figures 5 and 6.

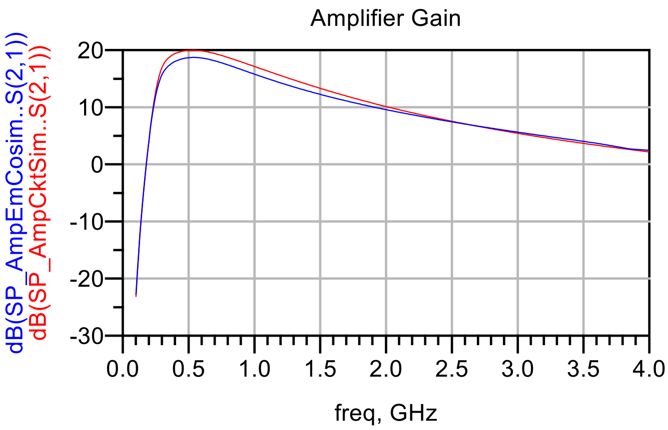

Figure 5. Amplifier Gain

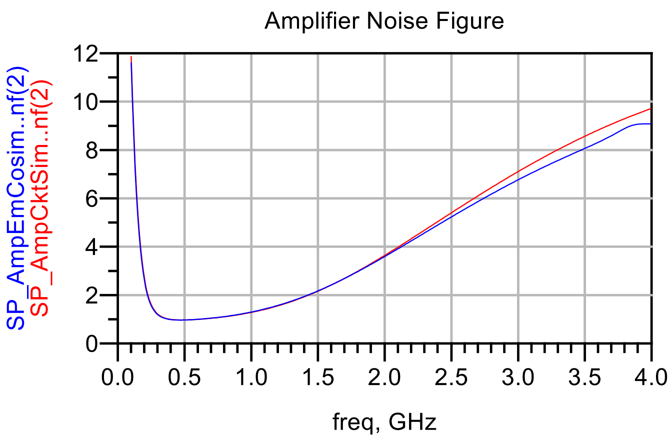

Figure 6. Amplifier Noise Figure

Figure 5 illustrates the S-parameter (S21) in dB, specifically showing the gain (forward transmission) of the LNA design as a function of frequency. The X-axis represents frequency, spanning the GHz spectrum. The Y-axis indicates the forward transmission coefficient (S21) measured in decibels (dB). The blue curve, labeled "dB(SP_AmpEmCosim_S(2,1))," represents the co-simulation EM results for S21, accounting for electromagnetic effects. In contrast, the red curve, labeled "dB(SP_AmpCktSim_S(2,1))," represents the circuit-level simulation of S21, excluding parasitic electromagnetic effects. Both curves exhibit a clear peak in S21, indicating the frequency at which the LNA provides maximum gain. This peak gain appears to be around 15-20 dB, which is a typical value for well-designed LNAs operating at 1 GHz.

At low frequencies, both the red and blue curves align closely. However, as the frequency approaches the peak, slight differences emerge between the two curves, suggesting that electromagnetic parasitics begin to influence gain. This difference may result from layout parasitics, such as coupling effects or losses in the physical design. After reaching the peak frequency, both curves decline, with the red curve dropping slightly more rapidly than the blue, indicating that the EM effects help maintain better gain performance at higher frequencies.

The gradual decrease in gain following the peak is expected, as LNAs are typically designed for optimal performance at specific frequencies—in this case, around 1 GHz. The co-simulation EM (blue curve) shows slightly better performance at higher frequencies. The LNA reaches its highest gain close to the target frequency, which shows that it amplifies signals well around 1 GHz

Figure 6 provides a more detailed analysis of the noise figure (NF) performance of LNA, simulated using the AT41411 transistor model. The X-axis indicates frequency, appearing to span the GHz range, consistent with the design target of 1 GHz. The Y-axis represents the noise figure in decibels (dB), which measures the amount of additional noise introduced by the amplifier relative to the theoretical minimum. Lower NF values signify better performance. The blue curve, labeled "SP_AmpEmCosim.nf(2)," represents the noise figure from the electromagnetic (EM) co-simulation, which incorporates layout and parasitic effects. The red curve, labeled "SP_AmpCktSim.nf(2)," shows the noise figure from the circuit-level simulation, excluding electromagnetic effects. At low frequencies, both curves align closely, indicating similar noise performance in both simulations, suggesting that parasitic effects may not significantly impact NF in this region. However, as the frequency increases towards 1 GHz, a slight difference arises, with the red curve showing a higher NF than the blue curve. This indicates that including layout effects in the EM simulation helps to reduce noise contributions, particularly at higher frequencies.

Near 1 GHz, the noise figure remains relatively low, which is desirable for low-noise amplifiers, indicating adequate signal amplification without introducing excessive noise. Beyond 1 GHz, the NF typically increases, reflecting the more pronounced effects of parasitics and frequency-dependent losses in practical circuit layouts. The noise figure of the LNA design at around 1 GHz is low, indicating good performance for low-noise amplifiers. This result is promising for applications requiring high signal integrity.

To relate the received signal power plot in Figure 2 from the two-ray model to the performance analysis of the LNA, particularly at around 1 GHz, where the received power is -77.31 dBm, the following reasoning can be followed. The two-ray model provides a framework for understanding the propagation characteristics of signals in a wireless communication environment. In this model, the received signal power is influenced by factors such as the distance between the transmitter and receiver, antenna heights, and the environment (e.g., reflections from the ground).

In the context of the LNA designed for an IoT water monitoring system, the received signal power of -77.31 dBm indicates a weak signal that the LNA must amplify to ensure adequate quality for further processing. Given the low received signal power, the LNA's performance becomes crucial. The gain of the LNA, which ranges from 15 to 20 dB, plays a vital role in boosting the received signal. For instance, if the LNA has a gain of 20 dB, it would increase the received power from -77.31 dBm to approximately -57.31 dBm, which compensates for the inherent losses in signal strength due to distance and environmental factors.

The noise figure of the LNA, which ranges from 2 to 3 dB, determines the amount of additional noise introduced to the signal during amplification. A low noise figure is critical when working with weak signals like -77.31 dBm to maintain signal integrity. The relationship between the received signal power and the LNA's performance can also be examined through impedance matching. The simulation results from the two-ray model highlight the need for the LNA to operate effectively at the specified frequency of around 1 GHz. The performance metrics, such as gain, noise figure, and stability, must be optimized to ensure that the LNA can handle the received power level efficiently.

5. Conclusions

Based on the performance analysis of the LNA, it can be concluded that electromagnetic (EM) simulation provides more accurate predictions regarding the reflection coefficients and noise figure at higher frequencies. At approximately 1 GHz, the EM simulation indicates a more significant reduction in the input reflection coefficient (S(1,1)) compared to the circuit simulation, suggesting improved impedance matching. The amplifier gain ranges from 15 to 20 dB, while the noise figure is measured between 2 and 3 dB, demonstrating good performance for low-noise amplifiers. Notable differences in performance are observed at low frequencies, attributed to parasitic effects that are not captured in the circuit simulation. Conversely, at high frequencies, these parasitic effects become more pronounced in the EM simulation. Future research should aim to enhance performance by refining the circuit layout, with a particular focus on improving impedance matching and transistor biasing.

Acknowledgment

The authors would like to express sincere gratitude to Universitas Lampung for the research funding provided through Contract No. 574/UN26.21/PM/2024. This support helped facilitate the successful completion of this research project.

References

1. P. Salunke and J. Kate, "Advanced smart sensor interface in internet of things for water quality monitoring," in 2017 International Conference on Data Management, Analytics and Innovation (ICDMAI), 2017.
2. V. Radhakrishnan and W. Wu, "IoT Technology for Smart Water System," in 2018 IEEE 20th International Conference on High Performance Computing and Communications, 2018.
3. J.-E. Frey, "WISA - wireless control in theory, practice and production," in 2008 IEEE International Conference on Emerging Technologies and Factory Automation, 2008.
4. D. G. Michelson and S. S. Ghassemzadeh, "Measurement and Modeling of Wireless Channels," in New Directions in Wireless Communications Research, Springer, 2009, pp. 1-27.
5. A. Takahashi, T. Saito, M. Ozawa and E. Shimizu, "Characteristic analysis of UHF band propagation channel form under the sea," in 2014 IEEE International Conference on Systems, Man, and Cybernetics (SMC), 2014.
6. K. G. Omeke, A. Abohmra, M. A. Imran, Q. H. Abbasi and L. Zhang, "Characterization of RF signals in different types of water," in Antennas and Propagation Conference 2019 (APC-2019), 2019.
7. H. Hitney, "Evaporation duct propagation and near-grazing angle scattering from a rough sea," in IEEE 1999 International Geoscience and Remote Sensing Symposium, 1999.
8. M. Fischer, M. Ferdik, L.-O. Rack, G. Saxl, M. Renzler and T. Ussmueller, "An Experimental Study on the Feasibility of a Frequency Diverse UHF RFID System," IEEE Access, vol. 7, pp. 132311-132323, 2019.
9. E. Bedeer, J. Pugh, C. Brown and H. Yanikomeroglu, "Measurement-Based Path Loss and Delay Spread Propagation Models in VHF/UHF Bands for IoT Communications," in 2017 IEEE 86th Vehicular Technology Conference (VTC-Fall), 2017.
10. A. E. Pallares-Calvo, B. E. Carvajal-Gámez and O. O. Gutiérrez-Frías, "Architecture of a Network of Low-Frequency Smart Sensors for IoT Applications in Marine Environments," in Late Breaking Posters. HCII 2022. Communications in Computer and Information Science, 2022.

11. A. Harun, D. L. Ndzi, M. F. Ramli, A. Y. M. Shakaff, M. N. Ahmad, L. M. Kamarudin, A. Zakaria and Y. Yang, "Signal Propagation in Aquaculture Environment for Wireless Sensor Network Applications," in Progress In Electromagnetics Research, 2012.
12. "Received Signal Strength Indication (RSSI) of 2.4 GHz and 5 GHz Wireless Local Area Network Systems Projected over Land and Sea for Near-Shore Maritime Robot Operations," Journal of Marine Science and Engineering, 2019.
13. V. Kirichenko, Y. Logvinov, Y. Pedenko and V. Razskazovskyy, "Multipath simulating model of the microwave propagation near the sea surface," in Fourth International Kharkov Symposium 'Physics and Engineering of Millimeter and Sub-Millimeter Waves, 2001.
14. A. Abou-Taleb and D. Cooper, "Microwave scattering by surface waves on water," IEEE Journal of Oceanic Engineering, vol. 11, no. 2, pp. 316-321, 1986.
15. A. Youssef and J. Haslett, "Wideband CMOS LNA Design Techniques. In: Nanometer CMOS RFICs for Mobile TV Applications," in Nanometer CMOS RFICs for Mobile TV Applications, Springer, 2010.
16. J. Liu, "Analysis of Low-Noise Amplifier," in 2021 6th International Conference on Intelligent Computing and Signal Processing (ICSP), 2021.
17. B. Lehmeyer, M. T. Ivrlač and J. A. Nossek, "LNA noise parameter measurement},," in 2015 European Conference on Circuit Theory and Design (ECCTD), 2015.
18. W. Namgoong and J. Lerdworatawee, IEEE Transactions on Circuits and Systems I: Regular Papers, vol. 51, no. 7, pp. 1330-1335, Noise figure of digital communication receivers-revisited.
19. A. Bose and S. Pezaris, "A Theorem Concerning Noise Figures," IRE Transactions on Circuit Theory, vol. 3, no. 3, pp. 190-196, 1956.